Postprint of: Nosko O., Hyperbolic heat conduction at a microscopic sliding contact with account of adhesion-deformational heat generation and wear, International Journal of Thermal Sciences, Vol. 137 (2019), pp. 101-109, DOI: 10.1016/j.ijthermalsci.2018.11.013

Hyperbolic heat conduction at a microscopic sliding contact with account of adhesion-deformational heat generation and wear

Oleksii Nosko

Bialystok University of Technology, Faculty of Mechanical Engineering,
ul. Wiejska 45C, Bialystok, 15-351, Poland
E-mail: o.nosko@pb.edu.pl

Different non-Fourier models were proposed to simulate temperatures in materials subjected to extremely fast thermal disturbances, when the speed of heat propagation should be concerned. The present study investigated temperature and heat balance at a microscopic sliding contact during a single frictional interaction based on the Cattaneo-Vernotte hyperbolic heat conduction equation. Two fundamental features of friction, namely, adhesion-deformational heat generation and wear, were taken into account. By applying the Laplace transform approach, non-stationary temperature expressions were derived for the hyperbolic and classical parabolic heat conduction equations. Parametric analysis was then done for parameter ranges typical of brake materials. It was found that the hyperbolic heat conduction generally results in a higher temperature at the sliding surface compared to the parabolic heat conduction. The influence of the heat propagation speed can be significant for thermal relaxation time of the order above microsecond. It becomes stronger with an increase in the contribution of the adhesive heat generation. Another finding obtained is that a considerable fraction of heat is removed from the contact zone along with wear debris, resulting in a lower temperature. This fraction is larger for the hyperbolic heat conduction.

Keywords: hyperbolic heat conduction, thermal relaxation time, sliding contact, friction heat generation, adhesion-deformational heat generation, wear

Notation

c	specific heat capacity
$\mathrm{erfc}(\cdot)$	complementary error function
g	volumetric heat-generation rate
h	mechanically affected layer thickness
k	thermal diffusivity, $k = K/(\rho c)$
$\lg(\cdot)$	logarithm to base 10
q	heat flux
$\bar{q}$	heat flux vector
q_0	specific power of heat generation
s	Laplace transform parameter
t	time variable / sliding duration
u	linear wear intensity
u_n	linear wear intensity of the nominal surface
x	spatial coordinate
$H(\cdot)$	Heaviside step function
$I_\upsilon(\cdot)$	modified Bessel function of the first kind of order υ
K	thermal conductivity
Q	dimensionless heat flux, $Q = q/q_0$
T	temperature
T_0	initial temperature
U	dimensionless wear intensity, $U = u\sqrt{\tau}/\sqrt{k}$
β	deformational heat-generation decay coefficient, $\beta = 2\sqrt{k\tau}/h$
η	dimensionless time variable / sliding duration, $\eta = t/(2\tau)$
ϑ	dimensionless temperature, $\vartheta = K(T - T_0)/\left(2q_0\sqrt{k\tau}\right)$
ϑ_p	dimensionless ‘parabolic’ temperature
ξ	dimensionless spatial coordinate, $\xi = x/\left(2\sqrt{k\tau}\right)$
ρ	density
τ	thermal relaxation time
ϕ	heat fraction removed with wear debris
ϕ_p	‘parabolic’ heat fraction removed with wear debris
ψ	adhesive heat-generation fraction
∇T	temperature gradient
$\mathcal{L}[\cdot]$	Laplace transform operator
$\widetilde{\blacksquare}$	Laplace transform image

1. Introduction

The classical *parabolic* heat conduction equation based on the Fourier law has been successfully employed for solving various problems of heat transfer. According to the Fourier law [1], a temperature gradient ∇T in a conductive medium causes an immediate heat flux $\bar{q}$, which implies infinite speed of heat propagation. Experiments showed that in materials with non-homogeneous structure thermal waves travel with finite speeds, and the parabolic heat conduction equation may not be applicable to accurately simulate such a behaviour (Kaminski [2], Mitra et al. [3], Roetzel et al. [4]). This equation fails to predict temperatures under extremely fast thermal disturbances induced, for instance, by a laser (Li et al. [5], Jiang [6], Banerjee et al. [7]) or a flash lamp (Both et al. [8]), which is also attributed to the finiteness of the heat propagation speed.

Different non-Fourier models have been proposed to remove the mentioned theoretical inconsistency of the Fourier law (Ván [9]). Of these, the Cattaneo-Vernotte model takes a predominant place due to its simplicity. The relationship between ∇T and $\bar{q}$ is defined as (Cattaneo [10], Vernotte [11], Luikov [12])

$$\bar{q} + \tau \frac{\partial \bar{q}}{\partial t} = -K \nabla T \tag{1}$$

where t is the time variable; K is the thermal conductivity; τ is the thermal relaxation time which represents the time lag between ∇T and $\bar{q}$. The heat propagation speed is directly related to τ and equals $\sqrt{k/\tau}$, where k is the thermal diffusivity. In the particular case $\tau = 0$, Eq.(1) transforms into the Fourier law. Combination of Eq.(1) and the statement of energy conservation for a volume element gives the *hyperbolic* heat conduction equation.

Thermal friction problems occupy an important niche among heat transfer problems. Whenever two bodies are in sliding motion, their mechanical energy is transformed into friction heat. The dissipation of the friction heat in the bodies results in an increase in their temperatures, which inevitably affects the thermo-mechanical and tribological characteristics. A thermal friction problem is usually formulated in the form of a problem of non-stationary heat conduction for one or both friction bodies (Yevtushenko and Kuciej [13]). If it is defined macroscopically, temperature distributions in the bodies are simulated with account of the thermal processes at their sliding interface and boundaries with the environment. On the other hand, if the main focus is on the thermo-mechanical interaction between rough surfaces in sliding, temperature is simulated for a microscopic contact zone including one or a few roughness asperities. Regardless of the problem formulation level (macroscopic or microscopic), the simulations are performed using the parabolic heat conduction equation.

Frictional interactions of roughness asperities occur in a random manner. In most engineering systems, the typical interaction duration is of the order 10^{-8} to 10^{-6} s, as reported by

Kragelskii [14]. The heat generation associated with such a short interaction induces an extremely fast local heating of either of the sliding surfaces, similarly to a short-pulse heating by a laser. Consequently, the question arises whether the speed of heat propagation affects temperatures at microscopic sliding contacts. This question is intimately related to determination of the application limits for the parabolic heat conduction equation.

When two asperities come into contact, adhesion bonds occur between their atoms and molecules. Multiple formation and destruction of the adhesion bonds is accompanied by intensive heat generation (adhesive heat generation). The interaction of the asperities is not limited to adhesion but also involves deformational processes (Rigney and Hirth [15], Kennedy [16]). Plastic deformations occur in the vicinity of the asperities, which is sometimes referred to as 'mechanically affected layer', and represent another source of heat (deformational heat generation). Since the adhesive heat generation occurs directly at the sliding interface, it is modelled by a concentrated heat source, e.g. prescribed heat fluxes. By contrast, the deformational heat generation is specified in the form of a volumetric heat source (Kennedy [17]). Thereby, accurate simulations should allow for both mentioned sources of heat.

During a frictional interaction, wear debris detaches from an asperity and carries some of the friction heat away. According to the principle of heat balance, this should lead to a reduction of the temperature in the asperity zone. Experiments on brake materials showed that the wear intensity u_{n} of the nominal surface is normally below 1 μm/s (Friedrich and Reinicke [18], Findik [19]), while the temperature gradient ∇T attains a maximum level of 0.1–1 °C/μm (Newcomb [20], Balakin [21]). The product $u_{\mathrm{n}} \times \nabla T$ can thus hardly reach a value of 1 °C/s, which implies that the wear process has insignificant effect on transient temperatures when considered macroscopically. The situation is drastically different for a single asperity. Since the total contact area of roughness asperities is by 2–3 orders of magnitude smaller than the nominal contact area (Bowden and Tabor [22], Myshkin et al. [23]), the asperity wear intensity is expected to be proportionally larger than u_{n}. Furthermore, as revealed by Rozeanu and Pnueli [24], ∇T at a microscopic contact is by 3 orders of magnitude larger compared to that at the nominal surface. This reasoning leads to the hypothesis that the wear process affects temperature in the asperity zone.

The purpose of the present study was to analytically investigate the influence of the heat propagation speed on the temperature and heat balance at a microscopic sliding contact during a single interaction with account of the above mentioned fundamental features of friction — adhesion-deformational heat generation and wear.

2. Mathematical model

Consider a semispace which initially occupies the domain $x > 0$ and moves with constant velocity u in the direction opposite to the x-axis. The semispace is heated by a volumetric heat source of rate g dependent on x. The temperature $T(x,t)$ and heat flux $q(x,t)$ in the semispace are then related by the following heat balance equation (Al-Khairy and AL-Ofey [25], Han and Peddieson [26]):

$$\rho c\left(\frac{\partial T(x,t)}{\partial t} - u\frac{\partial T(x,t)}{\partial x}\right) + \frac{\partial q(x,t)}{\partial x} = g(x) \tag{2}$$

where ρ is the density; c is the specific heat capacity.

Accepting a non-zero thermal relaxation time τ and taking the motion of the semispace into account allow expressing Eq.(1) in the form (Christov and Jordan [27])

$$q(x,t) + \tau\left(\frac{\partial q(x,t)}{\partial t} - u\frac{\partial q(x,t)}{\partial x}\right) = -K\frac{\partial T(x,t)}{\partial x} \tag{3}$$

Combination of Eqs.(2) and (3) yields the heat transport equation with respect to $q(x,t)$ as follows:

$$\tau\frac{\partial^2 q}{\partial t^2} + \frac{\partial q}{\partial t} - 2\tau u\frac{\partial^2 q}{\partial x \partial t} - u\frac{\partial q}{\partial x} - (k - \tau u^2)\frac{\partial^2 q}{\partial x^2} = -k\frac{\partial g}{\partial x} \tag{4}$$

where the thermal diffusivity $k = K/(\rho c)$.

To a first approximation, heat flux in the vicinity of an asperity being in the frictional interaction with a counter-asperity is assumed to be geometrically one dimensional (Archard [28]). This allows applying Eq.(4) for determining the heat flux $q(x,t)$ in the vicinity of an asperity subjected to wear under the fulfilment of the following conditions. The asperity zone is represented by the domain $x > 0$. The asperity sliding surface is the plane $x = 0$. The asperity wear is simulated by the motion of the semispace, and, accordingly, the parameter u is set equal to the linear wear intensity of the asperity. The relevant schematic is presented in Fig.1.

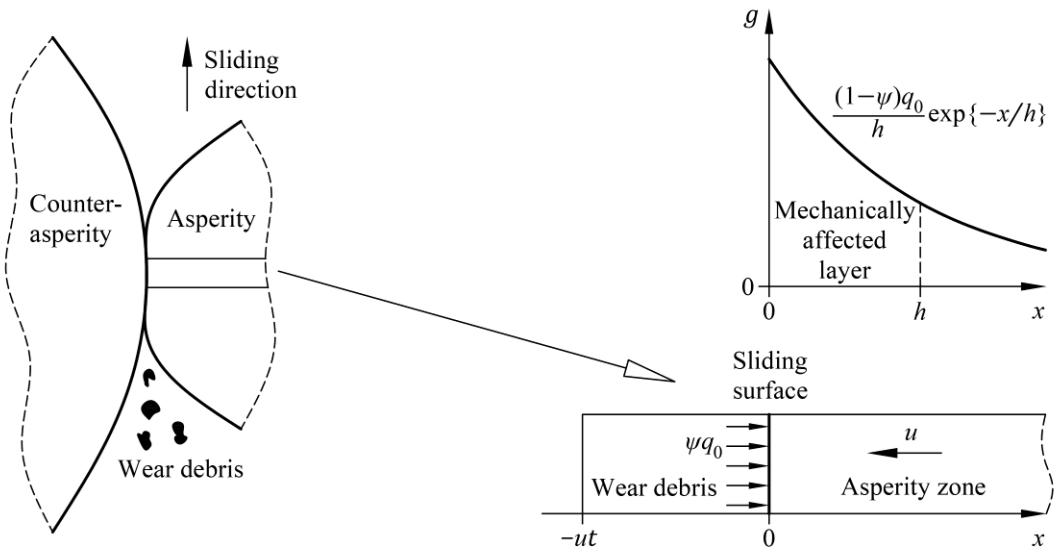

Fig.1. Schematic of the heat transport problem for an asperity zone (2-column image)

Let q_0 denote the quantity of heat generated per unit friction area per unit time. Assume that its fraction ψ is released at the sliding surface due to adhesion, while $(1-\psi)$ is released in the volume due to plastic deformations (Nosko [29]). Furthermore, based on the studies by Heilmann and Rigney [30] and Kennedy [16], the volumetric heat-generation rate g is assumed to decay exponentially with the distance x from the sliding surface. These assumptions allow describing the adhesive heat generation by the boundary condition

$$q|_{x=0} = \psi q_0 \tag{5}$$

and the deformational heat generation by the function

$$g(x) = \frac{(1-\psi)q_0}{h}\exp\left\{-\frac{x}{h}\right\} \tag{6}$$

where h is the thickness of the mechanically affected layer defined in the present study as the layer within which 63.2% of the 'deformational' friction heat is released.

The definition of the problem is completed by specifying zero heat flux at infinite distance from the sliding surface

$$q|_{x\to\infty} = 0 \tag{7}$$

and zero initial conditions

$$q|_{t=0} = \left.\frac{\partial q}{\partial t}\right|_{t=0} = 0 \tag{8}$$

Introduce the dimensionless spatial coordinate $\xi = x/\left(2\sqrt{k\tau}\right)$, time variable $\eta = t/(2\tau)$, heat flux $Q = q/q_0$, temperature $\vartheta = K(T-T_0)/\left(2q_0\sqrt{k\tau}\right)$, deformational heat-generation decay coefficient $\beta = 2\sqrt{k\tau}/h$, and wear intensity $U = u\sqrt{\tau}/\sqrt{k}$. Here T_0 is the initial temperature. This

allows decreasing the number of parameters in Eqs.(4)–(8) and writing the dimensionless heat transport equation with respect to $Q(\xi,\eta)$ in the form

$$\frac{\partial^2 Q}{\partial \eta^2}+2\frac{\partial Q}{\partial \eta}-2U\frac{\partial^2 Q}{\partial \xi \partial \eta}-2U\frac{\partial Q}{\partial \xi}-(1-U^2)\frac{\partial^2 Q}{\partial \xi^2}=(1-\psi)\beta^2\exp\{-\beta\xi\} \tag{9}$$

boundary conditions

$$Q|_{\xi=0}=\psi \tag{10}$$

and

$$Q|_{\xi\to\infty}=0 \tag{11}$$

and initial conditions

$$Q|_{\eta=0}=\left.\frac{\partial Q}{\partial \eta}\right|_{\eta=0}=0 \tag{12}$$

If the heat flux $Q(\xi,\eta)$ is known, the temperature $\vartheta(\xi,\eta)$ is derived using Eq.(3) written as

$$\vartheta(\xi,\eta)=\frac{1}{2}\int_{\xi}^{\infty}\left(2Q(\varsigma,\eta)+\frac{\partial Q(\varsigma,\eta)}{\partial \eta}\right)d\varsigma+\frac{U}{2}Q(\xi,\eta) \tag{13}$$

The problem defined by Eqs.(9)–(13) incorporates 3 parameters, namely, ψ, β and U.

It should be noted that the heat transport equation for an asperity zone can be formulated directly with respect to the temperature $T(x,t)$. However, the formulation of the boundary condition of Eq.(5) in terms of temperature and temperature gradient cannot be performed straightforward, as follows from Eq.(3), and requires application of the special mathematical methods (Yu et al. [31]).

3. Analytical solution

Application of the Laplace transform $\mathcal{L}$ to Eq.(9) with respect to η and taking account of Eq.(12) yield

$$(1-U^2)\frac{\partial^2 \tilde{Q}}{\partial \xi^2}+2U(s+1)\frac{\partial \tilde{Q}}{\partial \xi}-s(s+2)\tilde{Q}=-\frac{(1-\psi)\beta^2}{s}\exp\{-\beta\xi\} \tag{14}$$

where s is the transform parameter; $\tilde{Q}(\xi,s)$ is the image of $Q(\xi,\eta)$, i.e. $\tilde{Q}(\xi,s)=\mathcal{L}[Q(\xi,\eta)]$. Eq.(14) represents a non-homogeneous differential equation of the second order with exponential right side. Its general solution is

$$\begin{aligned}\tilde{Q}(\xi,s)=&A_1(s)\exp\left\{-\frac{\xi}{b}\left(U(s+1)-\sqrt{(s+1)^2-b}\right)\right\}\\&+A_2(s)\exp\left\{-\frac{\xi}{b}\left(U(s+1)+\sqrt{(s+1)^2-b}\right)\right\}+\frac{(1-\psi)\beta^2\exp\{-\beta\xi\}}{s(s+a_1)(s+a_2)}\end{aligned} \tag{15}$$

which incorporates two unknown functions $A_1(s)$ and $A_2(s)$ and the coefficients given by

$$a_1=1+\beta U-\sqrt{1+\beta^2};$$

$$a_2 = 1 + \beta U + \sqrt{1+\beta^2};$$
$$b = 1 - U^2$$

Under the assumption that $0 \le U < 1$, it follows from Eq.(11) that $A_1 = 0$. The other function is determined by substituting Eq.(15) into Eq.(10) in the space of images:

$$A_2(s) = \frac{\psi}{s} - \frac{(1-\psi)\beta^2}{s(s+a_1)(s+a_2)}$$

which allows rewriting Eq.(15) in the form

$$\tilde{Q}(\xi,s) = \left(\frac{\psi}{s} - \frac{(1-\psi)\beta^2}{s(s+a_1)(s+a_2)}\right)\exp\left\{-\frac{\xi}{b}\left(U(s+1)+\sqrt{(s+1)^2-b}\right)\right\} + \frac{(1-\psi)\beta^2\exp\{-\beta\xi\}}{s(s+a_1)(s+a_2)} \tag{16}$$

Substitution of Eq.(16) into Eq.(13) represented in the space of images as

$$\tilde{\vartheta}(\xi,s) = \mathcal{L}[\vartheta(\xi,\eta)] = \frac{s+2}{2}\int_{\xi}^{\infty}\tilde{Q}(\varsigma,s)\,d\varsigma + \frac{U}{2}\tilde{Q}(\xi,s)$$

yields

$$\tilde{\vartheta}(\xi,s) = \frac{1}{2}\left(\frac{\psi}{s} - \frac{(1-\psi)\beta^2}{s(s+a_1)(s+a_2)}\right)\left(\frac{b(s+2)}{U(s+1)+\sqrt{(s+1)^2-b}} + U\right) \times \exp\left\{-\frac{\xi}{b}\left(U(s+1)+\sqrt{(s+1)^2-b}\right)\right\} + \frac{(1-\psi)\beta\exp\{-\beta\xi\}(s+2+\beta U)}{2s(s+a_1)(s+a_2)}$$

or

$$\tilde{\vartheta}(\xi,s) = \tilde{\varphi}_1(\xi,s)\left(\tilde{\varphi}_2(s)\tilde{\varphi}_3(s) + \tilde{\varphi}_4(s)\right) + \tilde{\varphi}_5(\xi,s) \tag{17}$$

where

$$\tilde{\varphi}_1(\xi,s) = \exp\left\{-\frac{U\xi}{b}(s+1)\right\}\frac{\exp\left\{-\frac{\xi}{b}\sqrt{(s+1)^2-b}\right\}}{\sqrt{(s+1)^2-b}};$$
$$\tilde{\varphi}_2(s) = s+1-\sqrt{(s+1)^2-b};$$
$$\tilde{\varphi}_3(s) = \frac{U}{2s^2}\left(\psi - \frac{(1-\psi)\beta^2}{(s+a_1)(s+a_2)}\right);$$
$$\tilde{\varphi}_4(s) = \frac{(s+1)^2 - U(s+1) - b}{2s^2}\left(\psi - \frac{(1-\psi)\beta^2}{(s+a_1)(s+a_2)}\right) - \frac{\psi}{2};$$
$$\tilde{\varphi}_5(\xi,s) = \frac{\psi}{2}\tilde{\varphi}_1(\xi,s) + \frac{(1-\psi)\beta\exp\{-\beta\xi\}(s+2+\beta U)}{2s(s+a_1)(s+a_2)}$$

The original of $\tilde{\vartheta}(\xi,s)$ given by Eq.(17) is found using the convolution theorem for the Laplace transform:

$$\vartheta(\xi,\eta) = \int_0^{\eta}\varphi_1(\xi,\varsigma)\left(\int_0^{\eta-\varsigma}\varphi_2(\epsilon)\varphi_3(\eta-\varsigma-\epsilon)\,d\epsilon + \varphi_4(\eta-\varsigma)\right)d\varsigma + \varphi_5(\xi,\eta) \tag{18}$$

where $\varphi_i(\xi,\eta) = \mathcal{L}^{-1}[\tilde{\varphi}_i(\xi,s)]$, $i \in \{1,2,3,4,5\}$.

Transformation of $\tilde{\varphi}_1(\xi,s)$ according to

$$\mathcal{L}^{-1}[\tilde{\varphi}(s-a)] = \exp\{a\eta\}\,\varphi(\eta)$$

then

$$\mathcal{L}^{-1}[\exp\{-ds\}\,\tilde{\varphi}(s)] = \varphi(\eta-d)H(\eta-d)$$

and finally (Prudnikov et al. [32], p. 322)

$$\mathcal{L}^{-1}\left[\frac{\exp\left\{-d\sqrt{s^2-a^2}\right\}}{\sqrt{s^2-a^2}}\right] = I_0\left(a\sqrt{\eta^2-d^2}\right)H(\eta-d)$$

yields

$$\varphi_1(\xi,\eta) = \exp\{-\eta\}\,I_0\left(\sqrt{\frac{(b\eta-U\xi)^2-\xi^2}{b}}\right)H\left(\eta-\frac{\xi}{1-U}\right)$$

where $H(\cdot)$ is the Heaviside step function; $I_v(\cdot)$ is the modified Bessel function of the first kind of order v; $d > 0$.

The known transform (Carslaw and Jaeger [33], p. 495)

$$\mathcal{L}^{-1}\left[s-\sqrt{s^2-a^2}\right] = \frac{a\,I_1(a\eta)}{\eta}$$

allows finding the original of $\tilde{\varphi}_2(s)$ as follows:

$$\varphi_2(\eta) = \frac{\sqrt{b}}{\eta}\exp\{-\eta\}\,I_1\left(\sqrt{b}\,\eta\right)$$

The originals of $\tilde{\varphi}_3(s)$ and $\tilde{\varphi}_4(s)$ are obtained as

$$\varphi_3(\eta) = \frac{\psi U}{2}\eta + \frac{(1-\psi)\beta^2 U}{2}\left(\frac{a_1+a_2}{a_1^2a_2^2} - \frac{\eta}{a_1a_2} + \frac{\exp\{-a_1\eta\}}{a_1^2(a_1-a_2)} + \frac{\exp\{-a_2\eta\}}{a_2^2(a_2-a_1)}\right)$$

and

$$\begin{aligned}\varphi_4(\eta) = \frac{\psi}{2}&(2-U-U(1-U)\eta)\\ &-\frac{(1-\psi)\beta^2}{2}\left(\frac{(2-U)a_1a_2+U(1-U)(a_1+a_2)}{a_1^2a_2^2} - \frac{U(1-U)}{a_1a_2}\eta\right.\\ &+\frac{b-(1-a_1)^2+U(1-a_1)}{a_1^2(a_1-a_2)}\exp\{-a_1\eta\}\\ &\left.+\frac{b-(1-a_2)^2+U(1-a_2)}{a_2^2(a_2-a_1)}\exp\{-a_2\eta\}\right)\end{aligned}$$

The original of $\tilde{\varphi}_5(\xi,s)$ is given by

$$\varphi_5(\xi,\eta)=\frac{\psi}{2}\varphi_1(\xi,\eta)+\frac{(1-\psi)\beta}{2}\exp\{-\beta\xi\}\left(\frac{2+\beta U}{a_1a_2}+\frac{2-a_1+\beta U}{a_1(a_1-a_2)}\exp\{-a_1\eta\}+\frac{2-a_2+\beta U}{a_2(a_2-a_1)}\exp\{-a_2\eta\}\right)$$

Analysis of Eq.(18) should involve its comparison with a solution $\vartheta_{\mathrm{p}}(\xi,\eta)$ of the parabolic heat conduction problem incorporating equivalent volumetric heat source, boundary and initial conditions. This problem can be easily formulated by removing the terms associated with τ in Eqs.(9)–(13):

$$2\frac{\partial\vartheta_{\mathrm{p}}}{\partial\eta}-2U\frac{\partial\vartheta_{\mathrm{p}}}{\partial\xi}-\frac{\partial^2\vartheta_{\mathrm{p}}}{\partial\xi^2}=(1-\psi)\beta\exp\{-\beta\xi\};\quad -\left.\frac{\partial\vartheta_{\mathrm{p}}}{\partial\xi}\right|_{\xi=0}=\psi;\ \left.\frac{\partial\vartheta_{\mathrm{p}}}{\partial\xi}\right|_{\xi\to\infty}=0;\ \vartheta_{\mathrm{p}}\big|_{\eta=0}=0 \tag{19}$$

The Laplace transform approach and known transform (Prudnikov et al. [32], p.176, 192)

$$\mathcal{L}^{-1}\left[\frac{\sqrt{2s+a^2}-a}{2s}\exp\left\{-d\left(\sqrt{2s+a^2}+a\right)\right\}\right]=\frac{1}{\sqrt{2\pi\eta}}\exp\left\{-\frac{(d+a\eta)^2}{2\eta}\right\}-\frac{a}{2}\operatorname{erfc}\left\{\frac{d+a\eta}{\sqrt{2\eta}}\right\}$$

allow deriving the solution of Eq.(19) as follows:

$$\vartheta_{\mathrm{p}}(\xi,\eta)=\int_0^{\eta}\left(\frac{1}{\sqrt{2\pi\varsigma}}\exp\left\{-\frac{(\xi+U\varsigma)^2}{2\varsigma}\right\}-\frac{U}{2}\operatorname{erfc}\left\{\frac{\xi+U\varsigma}{\sqrt{2\varsigma}}\right\}\right)\times\left(\psi+\frac{(1-\psi)\beta}{\beta-2U}\left(1-\exp\left\{\beta\left(\frac{\beta}{2}-U\right)(\eta-\varsigma)\right\}\right)\right)d\varsigma-\frac{1-\psi}{\beta-2U}\exp\{-\beta\xi\}\left(1-\exp\left\{\beta\left(\frac{\beta}{2}-U\right)\eta\right\}\right) \tag{20}$$

where $\operatorname{erfc}(\cdot)$ is the complementary error function.

Although the temperature expressions ϑ and ϑ_{p} given by Eqs.(18) and (20) were found using the classical mathematical methods, they are additionally validated by comparisons with several known analytical expressions. Fig.2 shows the distributions of ϑ and ϑ_{p} and the values calculated from the hyperbolic heat conduction expressions by Yu et al. [31] and Lewandowska [34] and parabolic heat conduction expressions by Carslaw and Jaeger [33]. Solid and dashed lines stand for Eqs.(18) and (20), respectively. A perfect matching can be seen between the presented results.

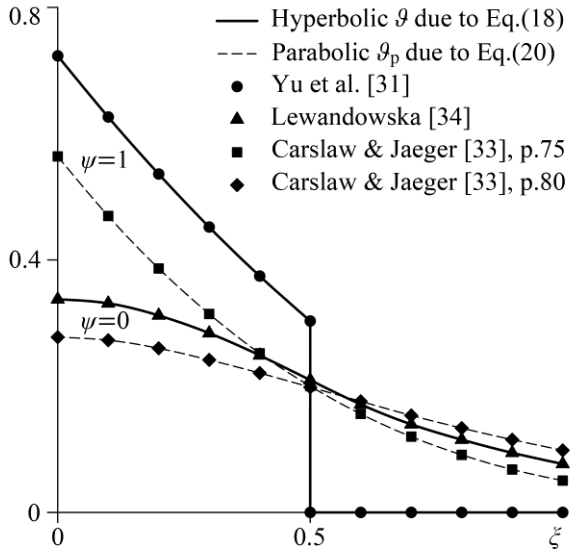

Fig.2. Validation of Eqs.(18) and (20) at η=0.5, β=2 and U=0 (1-column image)

4. Parameter variation ranges

Thermal relaxation time τ is the key parameter of the present study. Unfortunately, measurements of τ at normal and elevated temperatures are rare, and the relevant systematic data are not available. It is generally accepted that τ of metals is of the order 10^{-14} to 10^{-11} s (Özişik and Tzou [35]). By contrast, the experimental studies by Kaminski [2], Mitra et al. [3] and Roetzel et al. [4] showed that several materials with non-homogeneous structure, including sand, sodium bicarbonate and processed meat, have drastically larger τ of the order 10^{-1} to 10 s. A characteristic friction material comprises at least several non-metallic components of different origin and chemical composition. One can reasonably expect that τ of such a material exceeds 10^{-11} s. On the other hand, a value of the order 10^{-1} to 10 s looks to be a substantial overestimate of τ since no measurements were reported on deviations from the parabolic heat conduction in friction elements. Thus, τ of a multicomponent friction material most probably lies in the range 10^{-10} to 10^{-2} s.

Another important parameter is the asperity wear intensity u. As mentioned in the introduction, the nominal surface of a brake material is worn out with intensity u_n below 10^{-6} m/s. Assume that the total contact area of roughness asperities makes up 10^{-3} (i.e. 0.1%) of the nominal contact area, which agrees with the studies by Bowden and Tabor [22] and Myshkin et al. [23]. Then the maximum order of magnitude of u is estimated as $u_n \times 10^3 = 10^{-3}$ m/s.

Table 1 presents the estimated parameter variation ranges.

Table 1. Parameter variation ranges

Parameter	Minimum order of magnitude	Maximum order of magnitude
Thermal relaxation time τ, s	10^{-10}	10^{-2}
Sliding duration t, s [14]	10^{-8}	10^{-6}
Dimensionless sliding duration η	10^{-6}	10^{4}
Thermal diffusivity k, m^2/s	10^{-6}	10^{-4}
Mechanically affected layer thickness h, m [16]	10^{-7}	10^{-5}
Deformational heat-generation decay coefficient β	10^{-3}	10^{4}
Linear wear intensity u, m/s		10^{-3}
Dimensionless wear intensity U		10^{-1}

5. Results and discussion

5.1. Thermal wave

First consider the case of pure adhesive heat generation (ψ=1) in the absence of wear (U=0). Fig.3 shows the distributions of ϑ and ϑ_p at different values of η. It is seen that ϑ exceeds ϑ_p at the sliding surface ξ=0, i.e. the hyperbolic heat conduction results in a higher temperature compared to the parabolic heat conduction. The heat propagates in the form of a wave with a blunt front. According to Eq.(18), at each time instance η>0 the temperature ϑ undergoes a jump at the point $\xi = \eta$ from zero to the value of $\exp\{-\eta\}/2$. The propagation of similar thermal waves in a semispace was extensively studied theoretically (Glass et al. [36], Guillemet and Bardon [37]).

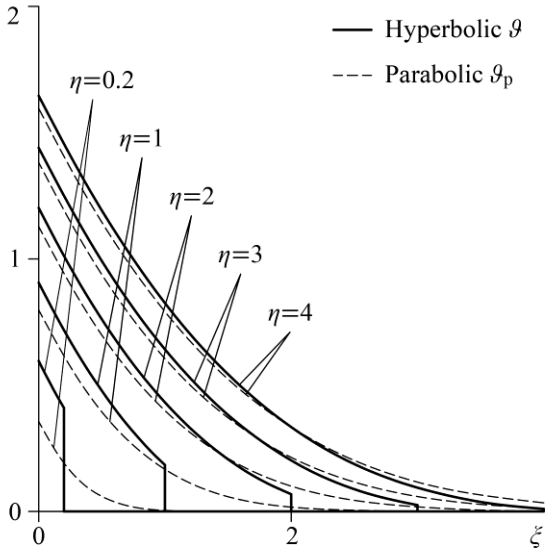

Fig.3. Distributions of the temperatures ϑ and ϑ_p at ψ=1 and U=0 (1-column image)

Figure 4 shows the evolution of ϑ and ϑ_p for different values of ξ. It is notable that there is an initial jump in ϑ at ξ=0, which is in contrast with the continuous curve of ϑ_p (Antaki [38], Zhang et al. [39]). Rapid temperature changes in the test samples subjected to an instantaneous heating were reported in a few experimental studies (Mitra et al. [3], Both et al. [8]). As concerns problems of friction, to the best author's knowledge, no hyperbolic heat conduction models were previously applied to characterising materials or simulating temperatures in engineering systems.

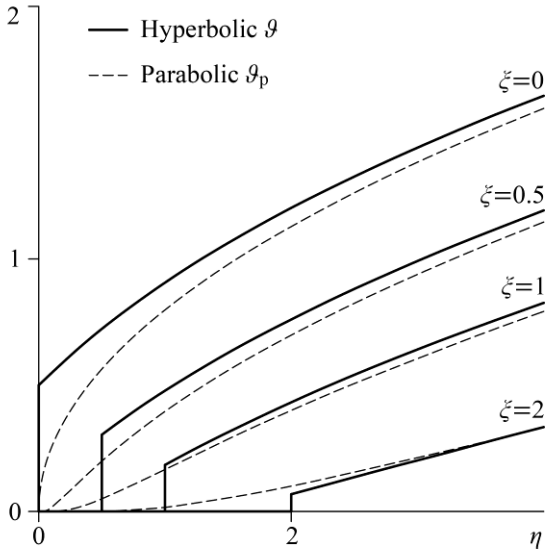

Fig.4. Evolution of the temperatures ϑ and ϑ_p at ψ=1 and U=0 (1-column image)

5.2. Adhesion-deformational heat generation

Figure 5 shows the distributions of ϑ and ϑ_p depending on the adhesive heat-generation fraction ψ. With a decrease in ψ, i.e. with a smaller contribution of the adhesive heat generation, ϑ and ϑ_p take smaller values at the sliding surface ξ=0, as does the difference $(\vartheta - \vartheta_p)$ characterising the influence of the heat propagation speed. The above mentioned jump in ϑ at $\xi = \eta$ also exhibits a tendency to decrease. In the case of pure deformational heat generation (ψ=0), ϑ has a continuous distribution. This implies that if plastic deformations are the predominant heat source, e.g. ψ<0.15 for copper-on-steel contact (Protasov and Kragelskii [40]), the absence of thermal waves with a blunt front cannot be considered as an evidence for the 'parabolic' nature of heat conduction.

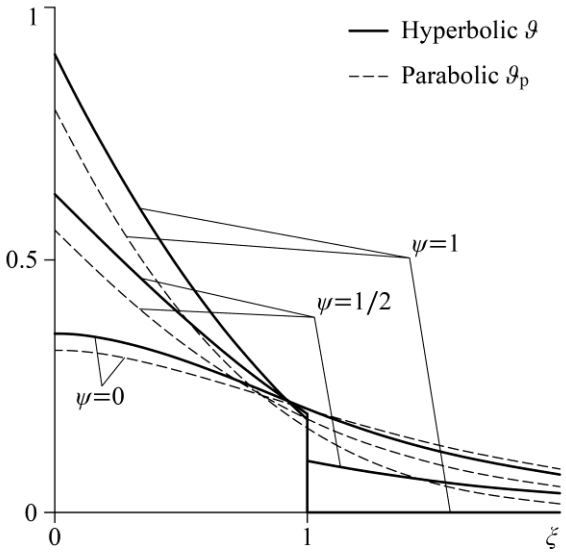

Fig.5. Influence of the adhesive heat-generation fraction ψ on the temperatures ϑ and ϑ_p at η=β=1 and U=0 (1-column image)

Figure 6 shows the influence of the deformational heat-generation decay coefficient β at ψ=0. At small values of β the difference $(\vartheta - \vartheta_p)$ is negligibly small, suggesting that the hyperbolic heat conduction can be neglected in favour of the parabolic heat conduction. With an increase in β, the deformational heat generation becomes more concentrated near ξ=0, which leads to higher temperatures ϑ and ϑ_p and larger difference $(\vartheta - \vartheta_p)$. This result agrees with those reported by Al-Khairy and AL-Ofey [25], Lewandowska [34], Yilbas et al. [41], Qi et al. [42], Talaee et al. [43].

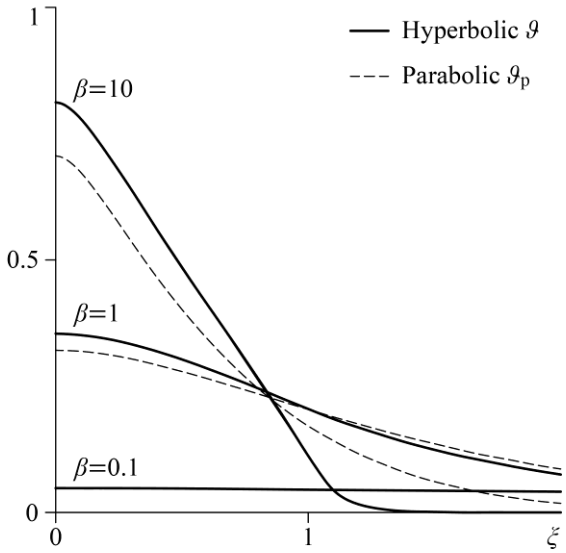

Fig.6. Influence of the deformational heat-generation decay coefficient β on the temperatures ϑ and ϑ_p at η=1 and ψ=U=0 (1-column image)

Parametric analysis of the temperatures ϑ and ϑ_{p} requires their comparisons with some reference temperature. The expression $\sqrt{2\,\eta/\pi}$ derived from Eq.(20) at ξ=U=0 and ψ=1 will serve for this purpose, which describes the dimensionless surface temperature of a parabolic heat conduction semispace of thermal conductivity K and diffusivity k heated at its surface by heat flux q_0 (Carslaw and Jaeger [33], p.75). The relative deviations ε and ε_{p} of the respective temperatures ϑ and ϑ_{p} from the reference temperature are then defined as follows:

$$\varepsilon(\eta) = \frac{\vartheta|_{\xi=0}}{\sqrt{2\,\eta/\pi}} - 1;$$

$$\varepsilon_{\mathrm{p}}(\eta) = \frac{\vartheta_{\mathrm{p}}|_{\xi=0}}{\sqrt{2\,\eta/\pi}} - 1$$

Figure 7 illustrates the behaviour of ε and ε_{p} for η varying from 10^{-4} to 10^{4} in logarithmic scale. At ψ=1 the deviation ε monotonically decreases to zero with increasing η. In general case, when ψ lies between 0 and 1 ($\psi = 1/2$ in Fig.7), ε changes its sign from positive to negative. This implies that the influence of the heat propagation speed, characterised by the difference $(\varepsilon - \varepsilon_{\mathrm{p}})$, is predominant at small values of η, while the influence of the deformational heat generation, characterised by $|\varepsilon_{\mathrm{p}}|$, predominates at larger η. As $\eta \to \infty$ it is true that $\vartheta|_{\xi=0} \sim \vartheta_{\mathrm{p}}|_{\xi=0} \sim \sqrt{2\,\eta/\pi}$, i.e. ε and ε_{p} are asymptotically equivalent.

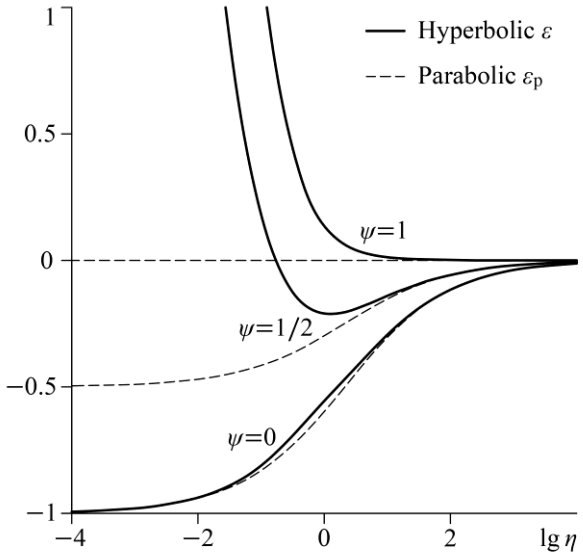

Fig.7. Influence of the adhesive heat-generation fraction ψ on the temperature deviations ε and ε_{p} at β=1 and U=0 (1-column image)

The curves of ε and ε_p have substantially different shapes when ψ=0. Fig.8 shows that ε practically coincides with ε_p at small values of β. With an increase in β, the influence of the heat propagation speed noticeably increases, which was also illustrated in Fig.6. Of interest is the fact that ε and ε_p exhibit an asymptotically equivalent behaviour at $\eta \to 0$, which is due to the relation $\vartheta|_{\xi=0} \sim \vartheta_p\big|_{\xi=0} \sim \beta\eta/2$ (Nosko [29]).

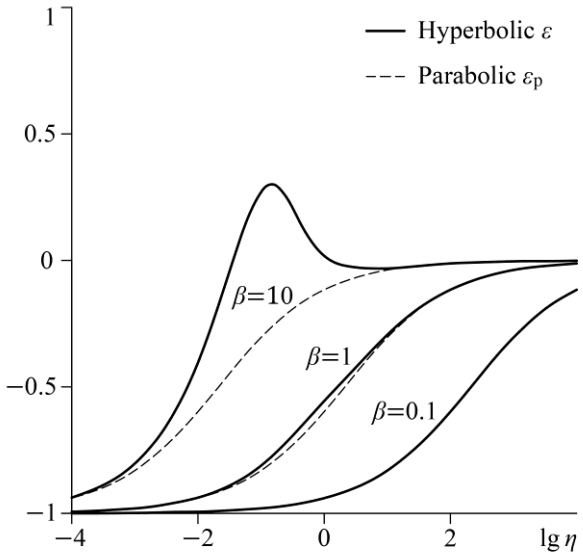

Fig.8. Influence of the deformational heat-generation decay coefficient β on the temperature deviations ε and ε_p at ψ=U=0 (1-column image)

Analysis of the simulation results including those presented in Figs.7 and 8 shows that the influence of the heat propagation speed is crucial at η of the order below 1, i.e. approximately at τ of the order above 10^{-6} s (see Table 1). This influence becomes stronger with increasing ψ or β.

5.3. Wear

Figure 9 shows the influence of the wear intensity U for ψ=1/2, when the adhesive and deformational processes contribute equally to heat generation. It is seen that an increase in U leads to a decrease in either of the temperatures ϑ and ϑ_p.

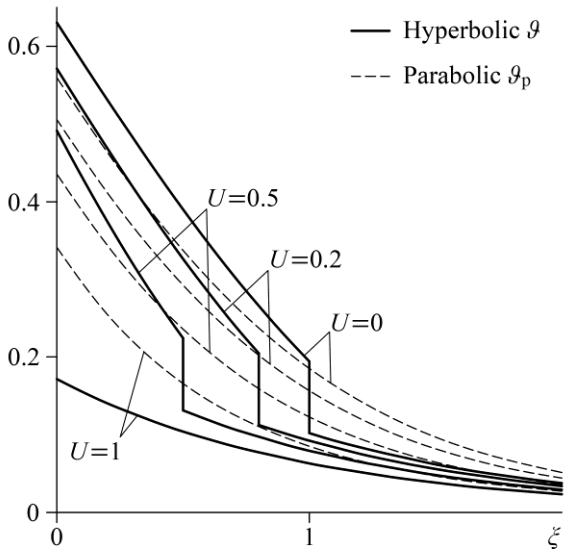

Fig.9. Influence of the wear intensity U on the temperatures ϑ and ϑ_p at η=β=1 and $\psi = 1/2$ (1-column image)

Of theoretical interest is the case $U \geq 1$ when the linear wear intensity u is equal to or greater than the heat propagation speed $\sqrt{k/\tau}$. Analysis of Eqs.(14) and (15) shows that in this case the heat flux image $\tilde{\vartheta}(\xi, s)$ is completely defined based on Eq.(11) without involving the boundary condition of Eq.(10) describing the adhesive heat generation. The corresponding temperature expression, which can be found from Eq.(18) by setting $\varphi_i(\xi, \eta) \equiv 0$, $i \in \{1,2,3,4\}$, is solely governed by the parameters of the deformational heat generation (see the curve of ϑ at $U = 1$ in Fig.9). Physically, this result is explained by that the surface layer affected by the adhesive heat generation is immediately worn out.

Figure 10 shows the deviations ε and ε_p calculated for pure adhesive heat generation (ψ=1) and different values of U. It is apparent that ε and ε_p monotonically decrease with η. There is, however, a qualitative difference in their behaviour at η of the order below 1, suggesting that the influence of the heat propagation speed predominates over that of wear. On the contrary, at η of the order above 1 the predominant process is wear, resulting in negative ε. As $\eta \to \infty$ both $\vartheta|_{\xi=0}$ and $\vartheta_p|_{\xi=0}$ tend to the stationary value of $1/(2U)$, which yields the asymptotic equivalence of ε and ε_p.

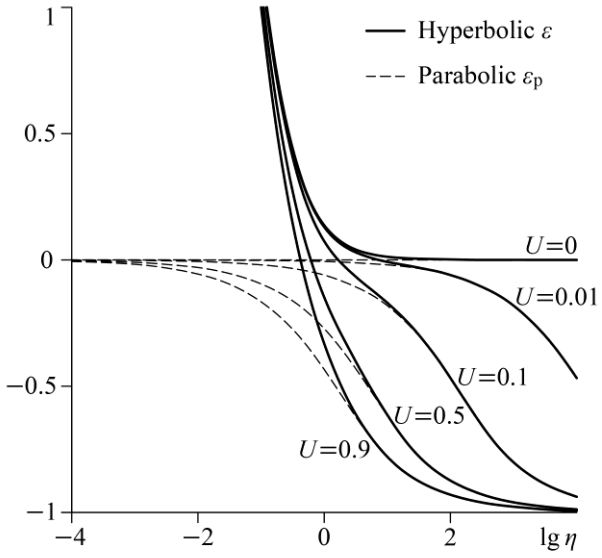

Fig.10. Influence of the wear intensity U on the temperature deviations ε and ε_{p} at ψ=1 (1-column image)

The temperature effect of wear should be analysed considering the heat balance in the asperity zone. With this in mind, introduce the quantities

$$\phi(\eta) = 1 - \frac{2}{\eta}\int_0^\infty \vartheta(\varsigma,\eta)d\varsigma$$

and

$$\phi_{\mathrm{p}}(\eta) = 1 - \frac{2}{\eta}\int_0^\infty \vartheta_{\mathrm{p}}(\varsigma,\eta)d\varsigma$$

which indicate the fractions of friction heat removed from the asperity zone with wear debris due to Eqs.(18) and (20), respectively.

Figure 11 shows the evolution of ϕ and ϕ_{p} at different values of U. Either of ϕ and ϕ_{p} monotonically increases with increasing η or U. It is remarkable that when $\eta \to 0$, ϕ tends to U, whereas ϕ_{p} tends to zero, which implies that wear debris carries away more heat in the case of the hyperbolic heat conduction. At η of the order above 1, ϕ and ϕ_{p} reach levels of several tens of percent, i.e. wear debris carries away a large amount of heat, which explains the reduction of the temperature deviations ε and ε_{p} illustrated in Fig.10. This result is of practical importance for U of the order below 10^{-1} (see Table 1). As $\eta \to \infty$ both ϕ and ϕ_{p} tend to 1.

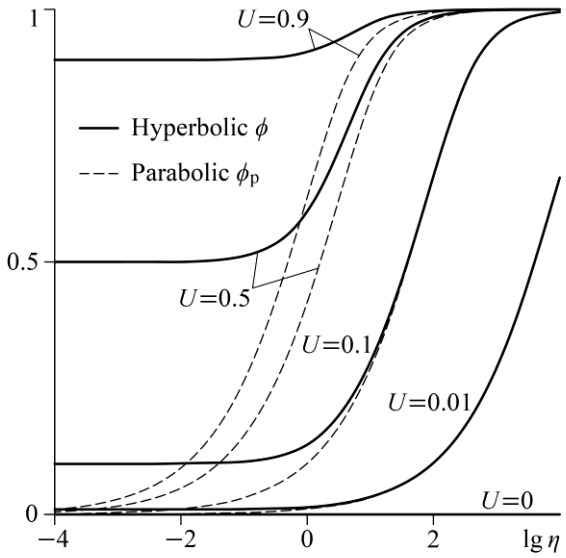

Fig.11. Influence of the wear intensity U on the heat fractions ϕ and ϕ_p removed with wear debris at ψ=1 (1-column image)

Several studies (Li et al. [44], Lin et al. [45], Chen et al. [46]) investigated frictional interactions between nanoscale metallic bodies using the method of Molecular Dynamics. This method involves numerical integration of the classical equations of motion for a system of atoms and allows simulating mechanical deformations and associated generation and dissipation of heat. It was shown that the friction of two metals is accompanied by extensive plastic deformations and material transfer, which results in the formation in the contact zone of a mixed layer. The studies by Lin et al. [45] and Chen et al. [46] revealed that the temperature at the boundary between the mixed layer and one or either of the metals is considerably lower than the maximum temperature in the mixed layer. One of the main causes for the temperature difference was concluded to be the motion of the boundary in the direction perpendicular to the initial sliding interface. This finding agrees qualitatively with that obtained in the present study stating that the wear of a sliding surface leads to its lower temperature. Thus, the formulae of Eqs.(18) and (20) can be potentially applied to simulating friction problems where the sliding interface motion is caused by a non-wear mechanism, such as material transfer.

Summarising the obtained findings, it should be underlined that the heat propagation speed is an important factor affecting the temperature and heat balance at microscopic sliding contacts. The extent of its influence can be significant at thermal relaxation time τ of the order above 10^{-6} s depending on the features of adhesion-deformational heat generation and wear. Further experimental studies are required here to determine τ of friction materials, which would enable more accurate simulations of thermal friction problems.

6. Conclusions

The influence of the finite speed of heat propagation on temperature and heat balance at a microscopic sliding contact was investigated with account of adhesion-deformational heat generation and wear. Based on the Laplace transform approach, the non-stationary temperature expressions of Eqs.(18) and (20) were derived for the Cattaneo-Vernotte hyperbolic heat conduction equation and classical parabolic heat conduction equation, respectively. Their parametric analysis led to the following findings:

1. Adhesion-deformational heat generation results in a thermal wave with a blunt front. Under pure deformational heat generation, the temperature distribution is continuous.
2. The hyperbolic heat conduction results in a higher temperature at the sliding surface compared to the parabolic heat conduction. The influence of the heat propagation speed can be significant at thermal relaxation time of the order above microsecond.
3. The influence of the heat propagation speed becomes stronger with an increase in the adhesive heat-generation fraction (ψ) or deformational heat-generation decay coefficient (β). The hyperbolic heat conduction can be neglected in favour of the parabolic heat conduction at pure deformational heat generation and small values of β.
4. An increase in the wear intensity (U) results in a temperature decrease, which is explained by that a considerable fraction of heat is removed from the contact zone with wear debris. This fraction is larger for the hyperbolic heat conduction.

The present work was supported by the National Science Centre, Poland [grant number 2017/26/D/ST8/00142].

References

[1] J. Fourier, Théorie analytique de la chaleur, F. Didot, Paris, 1822. (in French)

[2] W. Kaminski, Hyperbolic heat conduction equation for materials with a nonhomogeneous inner structure, Journal of Heat Transfer 112 (3) (1990) 555–560.

[3] K. Mitra, S. Kumar, A. Vedevarz, M.K. Moallemi, Experimental evidence of hyperbolic heat conduction in processed meat, Journal of Heat Transfer 117 (3) (1995) 568–573.

[4] W. Roetzel, N. Putra, S.K. Das, Experiment and analysis for non-Fourier conduction in materials with non-homogeneous inner structure, International Journal of Thermal Sciences 42 (2003) 541–552.

[5] J. Li, Y. Gu, Z. Guo, Analysis of the phenomena of non-Fourier heat conduction in switch-Q laser processing for reducing the core loss of grain-oriented silicon steel, Journal of Materials Processing Technology 74 (1998) 292–297.

[6] F. Jiang, Non-Fourier heat conduction phenomena in porous material heated by microsecond laser pulse, Microscale Thermophysical Engineering 6 (4) (2003) 331–346.

[7] A. Banerjee, A.A. Ogale, C. Das, K. Mitra, C. Subramanian, Temperature distribution in different materials due to short pulse laser irradiation, Heat Transfer Engineering 26 (8) (2005) 41–49.

[8] S. Both, B. Czél, T. Fülöp, G. Gróf, Á. Gyenis, R. Kovács, P. Ván, J. Verhás, Deviation from the Fourier law in room-temperature heat pulse experiments, Journal of Non-Equilibrium Thermodynamics 41 (1) (2016) 41–48.

[9] P. Ván, Theories and heat pulse experiments of non-Fourier heat conduction, Communications in Applied and Industrial Mathematics 7 (2) (2016) 150–166.

[10] C. Cattaneo, A form of heat conduction equation which eliminates the paradox of instantaneous propagation, Comptes Rendus 247 (1958) 431–433.

[11] P. Vernotte, Les paradoxes de la theorie continue de l'equation de la chaleur, Comptes Rendus 246 (1958) 3154–3155.

[12] A.V. Luikov, Thermal conductivity and diffusion, Gizlegprom, Moscow, 1941. (in Russian)

[13] A.A. Yevtushenko, M. Kuciej, One-dimensional thermal problem of friction during braking: The history of development and actual state, International Journal of Heat and Mass Transfer 55 (2012) 4148–4153.

[14] I.V. Kragelskii, Friction and Wear, Butterworths, London, 1965.

[15] D.A. Rigney, J.P. Hirth, Plastic deformation and sliding friction of metals, Wear 53 (1979) 345–370.

[16] F.E. Kennedy, Single pass rub phenomena — analysis and experiment, Journal of Lubrication Technology 104 (4) (1982) 582–588.

[17] F.E. Kennedy, Thermal and thermomechanical effects in dry sliding, Wear 100 (1984) 453–476.

[18] K. Friedrich, P. Reinicke, Friction and wear of polymer-based composites, Mechanics of Composite Materials 34 (6) (1998) 503–514.

[19] F. Findik, Latest progress on tribological properties of industrial materials, Materials and Design 57 (2014) 218–244.

[20] T.P. Newcomb, Transient temperatures in brake drums and linings, Proceedings of the Institution of Mechanical Engineers: Automobile Division 12 (1958) 227–244.

[21] V.A. Balakin, Heat-flow distribution and combined heat-mass transfer processes at the contact interface of a friction pair, Journal of Engineering Physics 40 (6) (1981) 660–665.

[22] F.P. Bowden, D.Tabor, The area of contact between stationary and between moving surfaces, Proceedings of the Royal Society A 169 (1939) 391–413.

[23] N.K. Myshkin, M.I. Petrokovets, A.V. Kovalev, Tribology of polymers: Adhesion, friction, wear, and mass-transfer, Tribology International 38 (2005) 910–921.

[24] L. Rozeanu, D. Pnueli, Two temperature gradients model for friction failure, Journal of Lubrication Technology 100 (1978) 479–485.

[25] R.T. Al-Khairy, Z.M. AL-Ofey, Analytical solution of the hyperbolic heat conduction equation for moving semi-infinite medium under the effect of time-dependent laser heat source, Journal of Applied Mathematics (2009) 604695.

[26] S. Han, J. Peddieson, Non-Fourier heat conduction/convection in moving medium, International Journal of Thermal Sciences 130 (2018) 128–139.

[27] C.I. Christov, P.M. Jordan, Heat conduction paradox involving second-sound propagation in moving media, Physical Review Letters 94 (2005) 154301.

[28] J.F. Archard, The temperature of rubbing surfaces, Wear 2 (1958/59) 438–455.

[29] O. Nosko, Partition of friction heat between sliding semispaces due to adhesion-deformational heat generation, International Journal of Heat and Mass Transfer 64 (2013) 1189–1195.

[30] P. Heilmann, D.A. Rigney, An energy-based model of friction and its application to coated systems, Wear 72 (1981) 195–217.

[31] Y.J. Yu, C.-L. Li, Z.-N. Xue, X.-G. Tian, The dilemma of hyperbolic heat conduction and its settlement by incorporating spatially nonlocal effect at nanoscale, Physics Letters A 380 (2016) 255–261.

[32] A.P. Prudnikov, Yu.A. Brychkov, O.I. Marichev, Integrals and series. Volume 4. Direct Laplace transforms, Gordon and Breach Science Publishers, New York, 1992.

[33] H.S. Carslaw, J.C. Jaeger, Conduction of heat in solids, 2nd ed., Oxford University Press, London, 1959.

[34] M. Lewandowska, Hyperbolic heat conduction in the semi-infinite body with a time-dependent laser heat source, Heat and Mass Transfer 37 (2001) 333–342.

[35] M.N. Özişik, D.Y. Tzou, On the wave theory in heat conduction, Journal of Heat Transfer 116 (3) (1994) 526–535.

[36] D.E. Glass, M.N. Özişik, D.S. McRae, Hyperbolic heat conduction with temperature-dependent thermal conductivity, Journal of Applied Physics 59 (6) (1986) 1861–1865.

[37] P. Guillemet, J.-P. Bardon, Conduction de la chaleur aux temps courts: les limites spatio-temporelles des modèles parabolique et hyperbolique, International Journal of Thermal Sciences 39 (2000), 968–982. (in French)

[38] P.J. Antaki, Analysis of hyperbolic heat conduction in a semi-infinite slab with surface convection, International Journal of Heat and Mass Transfer 40 (1997) 3247–3250.

[39] H. Zhang, Y. Zhang, H. Zhao, Non-Fourier heat conduction effects during high-energy beam metalworking, Tsinghua Science and Technology 9 (5) (2004) 596–600.

[40] B.V. Protasov, I.V. Kragelskii, On heat generation in external friction, Journal of Friction and Wear 2 (1982) 1–6.

[41] B.S. Yilbas, A.Y. Al-Dweik, S. Bin Mansour, Analytical solution of hyperbolic heat conduction equation in relation to laser short-pulse heating, Physica B 406 (2011) 1550–1555.

[42] H.-T. Qi, H.-Y. Xu, X.-W. Guo, The Cattaneo-type time fractional heat conduction equation for laser heating, Computers and Mathematics with Applications 66 (2013) 824–831.

[43] M.R. Talaee, A. Kabiri, R. Khodarahmi, Analytical solution of hyperbolic heat conduction equation in a finite medium under pulsatile heat source, Iranian Journal of Science and Technology, Transactions of Mechanical Engineering 42 (3) (2018) 269–277.

[44] B. Li, P.C. Clapp, J.A. Rifkin, X.M. Zhang, Molecular dynamics calculation of heat dissipation during sliding friction, International Journal of Heat and Mass Transfer 46 (2003) 37–43.

[45] E.-Q. Lin, L.-S. Niu, H.-J. Shi, Z. Duan, Molecular dynamics simulation of nano-scale interfacial friction characteristic for different tribopair systems, Applied Surface Science 258 (2012) 2022–2028.

[46] K. Chen, L. Wang, Y. Chen, Q. Wang, Molecular dynamics simulation of microstructure evolution and heat dissipation of nanoscale friction, International Journal of Heat and Mass Transfer 109 (2017) 293–301.